PAPER • **OPEN ACCESS**

Static Testing Using OFDR-based Quasi Continuous Fiber Optic Strain Sensing on the WiValdi Wind Turbine Rotor Blade

Journal of Physics: Conference Series **2767** (2024) 042005 doi:10.1088/1742-6596/2767/4/042005

Static Testing Using OFDR-based Quasi Continuous Fiber Optic Strain Sensing on the WiValdi Wind Turbine Rotor Blade

J Knebusch[1*], J Gundlach[1], D Meier[1], T Meier[1] and Y Govers[1]

[1]German Aerospace Center (DLR), Bunsenstr. 10, 37073 Göttingen, Germany
*johannes.knebusch@dlr.de

Abstract. The German research wind farm WiValdi was taken into service in 2023 and enables researchers and industry to conduct full-scale experiments. It currently consists of two highly instrumented wind turbines and multiple wind measurement masts. In one of the six wind turbine rotor blades, four Fiber Optic Strain Sensors (FOSS) are installed [1].
The strain which a wind turbine rotor blade exhibits under load is a key factor in the design, the certification and the assessment of its remaining service life as well as its further development and optimization. The aerodynamic optimization of wind turbine rotor blades leads to longer, and increasingly slender rotor blades and therefore increasingly relevant static and dynamic structural mechanical challenges.
Usually the strain of wind turbine rotor blades during static deflection tests is measured with electrical strain gauges (SGs) or Fiber-Bragg-Gratings (FBGs). In the present study, quasi-continuous Fiber-Optic-Strain-Sensors (FOSS) are used in parallel with FBGs. The underlying technology is called optical frequency domain reflectometry (OFDR) and since only glass-fibers are used, it is inherently lightning protected [2]. Besides that, it is commercially available and delivers strain results at a spatial resolution of 2.6 mm. For this study, there are four 50-meter-long glass fibers bonded to the wind turbine rotor blade on suction and pressure side of each main spar of a 57 m rotor blade. This contribution shows how the FOSS measurements are post-processed and validated. The validated data is then used to obtain the relation between strain and introduced force over the length of each FOSS. With the accurate prediction of root-bending-moments, one of many possible use-cases of the FOSS results, is presented.
Besides the computational model updating of the corresponding Finite-Element model in future investigations, the results will also be used to judge the current structural mechanical state of the wind turbine rotor blade at recurring service inspections. In that, results of the then to be acquired state at a given time and the shown base-line state will be compared. This will lead to high resolution insight into the deterioration of the structural integrity of the wind turbine rotor blade over time.
Considering that standard telecommunication glass fibers can be used as sensors, the cost per sensor (i.e. fiber) is relatively low (circa 1500 € for 50 m). Despite the high cost of the required measurement system, the low prices of the fibers make FOSS measurements not only a scientifically interesting but also a potentially economically viable solution for measuring strain on wind turbine rotor blades.

1. Introduction

The German research wind farm WiValdi, which was taken into service in 2023, allows researchers and industry to conduct large-scale experiments [1]. The facility is currently comprised of two highly

instrumented wind turbine generators and several wind measurement masts. Additionally, four fiber optic strain sensors (FOSS) have been installed in one of the six rotor blades of the wind turbine. These sensors deliver very high-resolution strain data, which is relevant in many regards. When certifying and estimating the remaining service life of a wind turbine rotor blade as well as when considering its future development and optimization, the strain which the wind turbine rotor blade exhibits under load is of crucial consideration. The aerodynamic optimization of wind turbine rotor blades results in longer, slender wind turbine rotor blades. These slender structures pose static and dynamic structural mechanical difficulties. Understanding the structural mechanical behavior in general and the stress-strain relation in particular is therefore important. FOSS deliver the quasi-continuous strain results [2], these results help in addressing the described challenges.

2. Measurements and test-setup

The WiValdi wind turbine rotor blade was tested under several different static load cases in 2022 by the Fraunhofer IWES in Bremerhaven, Germany. The herein investigated load cases are shown schematically in **Figure 1**. The description indicates which side of the wind turbine rotor blade is under compression and which side of the wind turbine rotor blade is under tension.

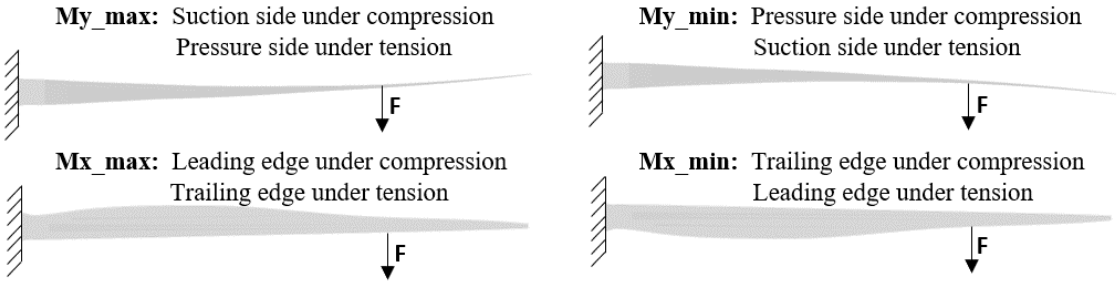

Figure 1. Setup for different load cases, wind turbine rotor blade is rotated accordingly

Photos of the static test-setup are shown in **Figure 2**. One can see the blue load-frames. In the different load cases, the rotor blade is rotated accordingly and then pulled towards the ground using a single load frame. The force is attacking in the shear center in flap wise (My_min, My_max) and edge wise (Mx_min, Mx_max) direction. The results generated from the loads acting on the fifth load frame (LF5) serve as a main reference in this publication. The results from the loads induced at the other four load frames (LF1 – LF4) are used to demonstrate that the reference data has a predictive character.

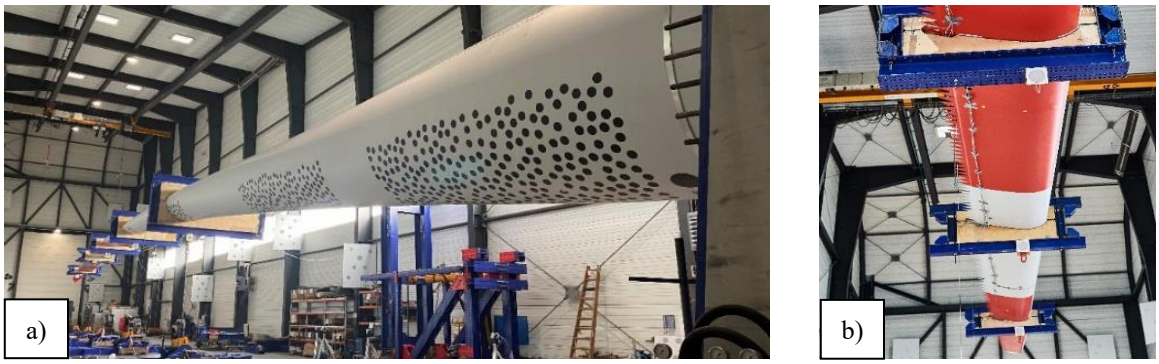

Figure 2. Exemplary static test-setup (a) My_Min | b) My_max)

Usually the strain of wind turbine rotor blades during static deflection tests is measured with electrical strain gauges (SGs) or Fiber-Bragg-Gratings (FBGs). In the present study, quasi-continuous Fiber-Optic-Strain-Sensors (FOSS) are used in parallel with FBGs. In Fiber Optic Strain Sensing, laser light

is sent through a glass fiber which is bonded to the structure i.e. the wind turbine rotor blade. Using a Mach-Zehnder Interferometer and a reference fiber, the Rayleigh-Backscatter of this laser-light creates a characteristic pattern in frequency domain. The change of this pattern under load is proportional to the strain experienced by the fiber and thus the strain of the wind turbine rotor blade. This technology is called optical frequency domain reflectometry (OFDR) and since only glass fibers and no wires are used on the structure, it is inherently lightning protected. It is commercially available at LUNA Innovations [2] and delivers strain results, like SGs or FBGs but with a quasi-continuous spatial resolution of 2.6 mm. For this study, there are four Fiber-Optic-Strain-Sensors (FOSS) bonded to the 57 m WiValdi wind turbine rotor blade. The FOSS are located on suction and pressure side of each main spar from the root towards the tip and are each approximately 50 m long. The location of the FOSS is shown in **Figure 3**. In **Figure 3** a) an isometric view of the FOSS locations on the geometry of the rotor blade is illustrated. The colors indicate the respective location of the FOSS. One can see from the front view in the bottom, in clockwise direction the turquoise fiber is located on the pressure side towards the trailing edge (TE_PS), the red fiber is located on the pressure side towards the leading edge (LE_PS), the orange fiber is located on the suction side towards the leading edge (LE_SS) and the blue fiber on the suction side towards the trailing edge (TE_SS). The colors and names which are used to indicate the locations of the Fiber Optic Strain Sensors (FOSS) are also used in the following to plot the results of the respective Fiber Optic Strain Sensor over the spanwise position of the wind turbine rotor blade. Subsequently, the FOSS are also referred to as “fibers”.
Besides the FOSS, there are FBGs mounted between the two main spars on the girder. Chord-wise they are located between the respective Leading Edge and Trailing Edge fiber. Their location is marked in black **Figure 3** a). The black markers are also used to plot the respective FBG results.

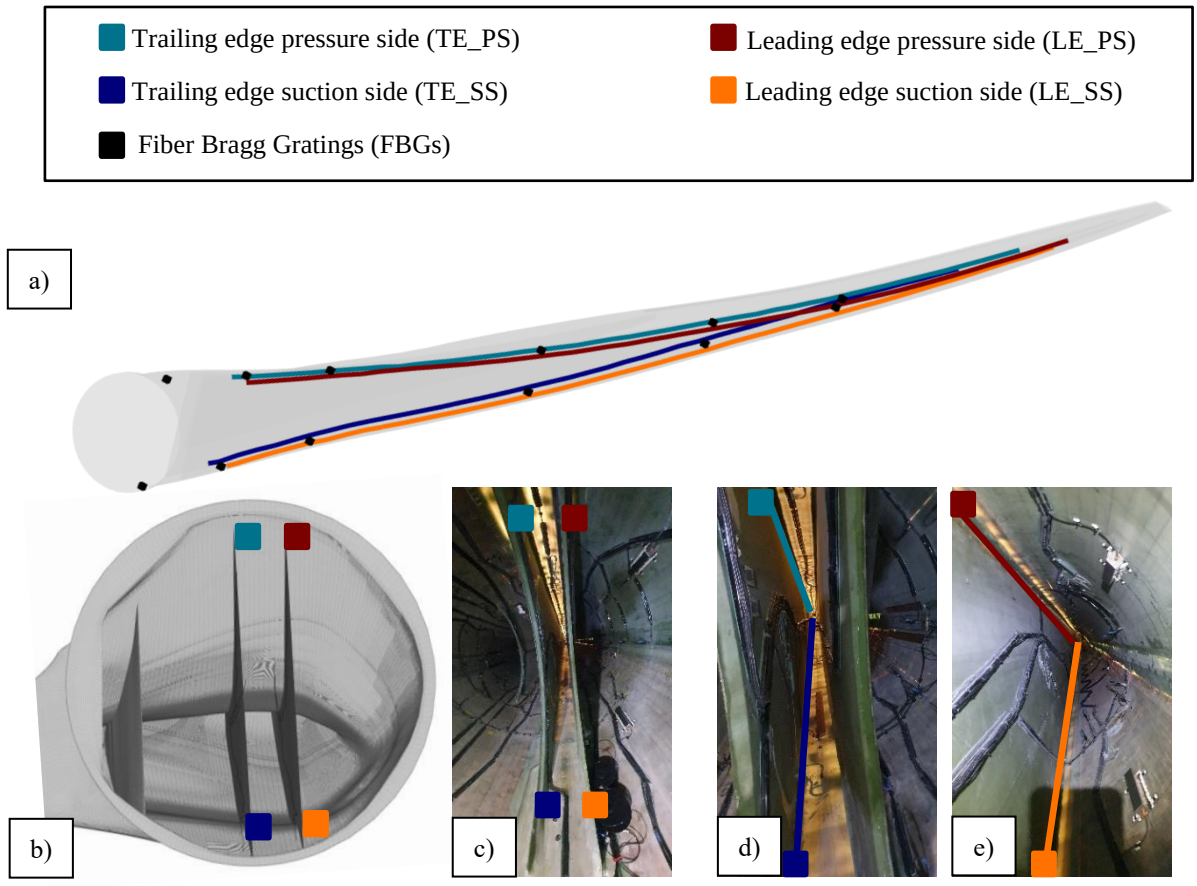

Figure 3. Sensor locations (a) iso view | b) front view | c) front view 2 | d) side view | e) side view 2)

3. Results and interpretation

3.1 Validation of FOSS data

In each of the load cases, the Force is increased and decreased in steps over time. An example of this is shown by the yellow line in Figure 4**.** This figure also shows the averaged strain response of one (out of approximately 19000) FOSS gauges over the measurement time (red line).

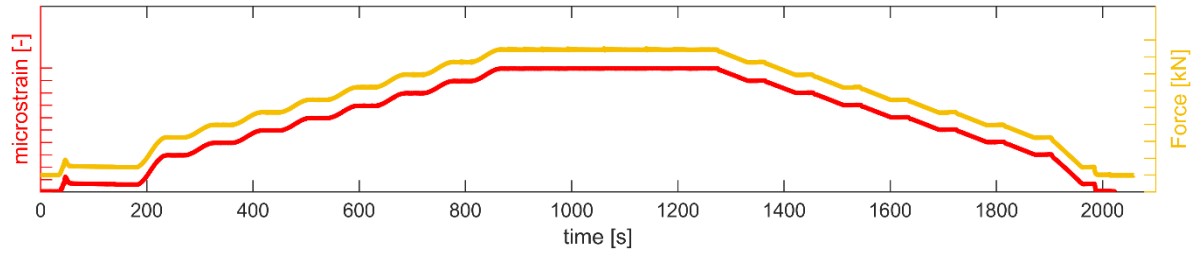

Figure 4. Exemplary load steps with introduced force and response of select FOSS over time

The results shown in the following each focus on a single time step, while giving high resolution spatial information over the length of each FOSS. The single time-step shown in the following is the time-step at which the force is highest (in this case at approximately 1050 s). While the spatial resolution of Fiber Optic Strain Sensors (FOSS) is very high, FOSS measurement data requires further post-processing to be meaningful and reliable [3,4,5]. In a first step, outliers in the strain results which are caused by known and physically explainable effects are omitted. This is the case for regions in which the fibers could not be perfectly bonded to the wind turbine rotor blade, because of construction limitations. It also required in regions in which the load frames lead to locally distorted results. Aside from deleting these outliers and linearly interpolating the remaining results, FOSS data requires additional treatment. **Figure 5** shows example FOSS data, for the load case My_Max, to illustrate why further post-processing is necessary. The results at highest force for the LE_PS fiber are plotted over the spanwise position (zoomed into 22 m to 23 m). In this, the light dashed red line is used for the original data. Furthermore, three exemplary spanwise regions are highlighted with blue, black and green dashed lines. The blue dashed line highlights spanwise positions at which no measurement data was acquired in the respective time step. The black dashed line highlights a region in which the difference in strain between subsequent positions is large. Part of the results in this black region are considered to be questionable, because the measured strain varies by over 70 microstrain over a length of 5.2 mm (Spanwise position of approx. 22.5 m). The green dashed line highlights a region in which the variance is large. These three types of measurement irregularities are partly caused by the measurement system itself and partly by how the fiber is glued to the wind turbine rotor blade. While the connection between fiber and rotor blade is generally considered very good it is locally imperfect. At those locations, the forces are not completely transferred from the wind turbine rotor blade to the fiber and therefore the measured values are not representative of the actual strain. The irregularities are uncommon for classical measurement techniques like Strain Gauges and ought to eliminated.

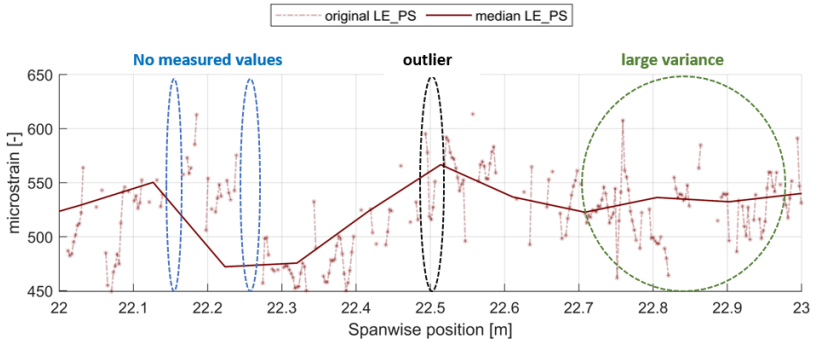

Figure 5. Exemplary original FOSS data with measurement irregularities and median of FOSS data

The elimination of these irregularities is achieved by spatially averaging the FOSS strain results of each 50 m fiber on 10 cm sections. In the example, the result of the averaging (i.e. the median) is shown with the dark red line (**Figure 5**). While the averaging reduces the spatial resolution (from 19 000 to 500 measuring points over a fiber length of 50 m) this still delivers strain results at a resolution that would be unfeasible with classical measurement techniques like SGs or FBGs. The section length of 10 cm is not universally viable but has to be chosen suitably for each structure. The aim is to average out measurement errors while retaining the characteristic strain response of the structure to the given load [5]. In the process of averaging, not only mean, but also median, standard deviation, skewness and kurtosis are calculated for every 10 cm section.
These results are then compared in order to ensure, that the averaging delivers meaningful results.
In the top of **Figure 6** the steps from the original data, to the validated data are shown in a flow chart. The bottom of **Figure 6** lists features of the original FOSS data as well as statistical methods to arrive at the validated FOSS data.

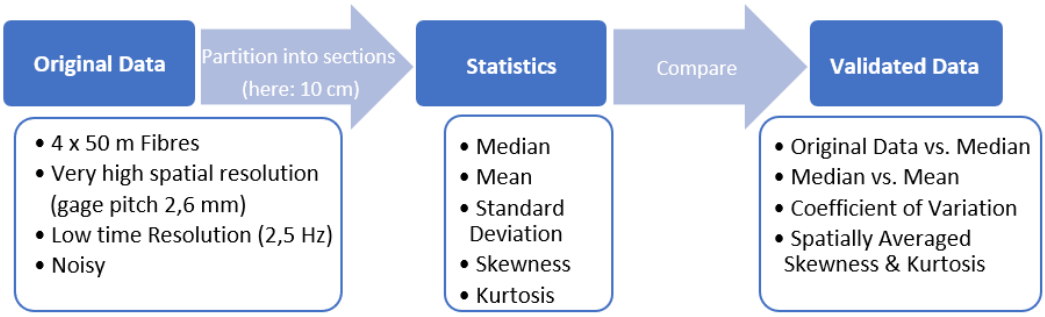

Figure 6. Use of statistics to turn original data into validated data

For the presented four reference load cases (My_Max, My_Min, Mx_Max, Mx_Min), the steps of this process are shown in the following. Here and in the following, the color of the lines corresponds to the respective FOSS (LE_PS, LE_SS, TE_PS, TE_SS). At first, the original data (light dots) is compared to the median (dark lines) for all load cases (**Figure 7**). The straight, non-varying, lines (e.g. at a spanwise position of 31 m) in the result plot are due to the previously explained linear interpolation. Apart from this, there is generally a large variance in the original data. However, the original data does not appear to be skewed and is in that regard well represented by the median (**Figure 7**). This impression is confirmed, when overlaying mean (light lines) and median (dark dashed lines), which are very similar (**Figure 8**).

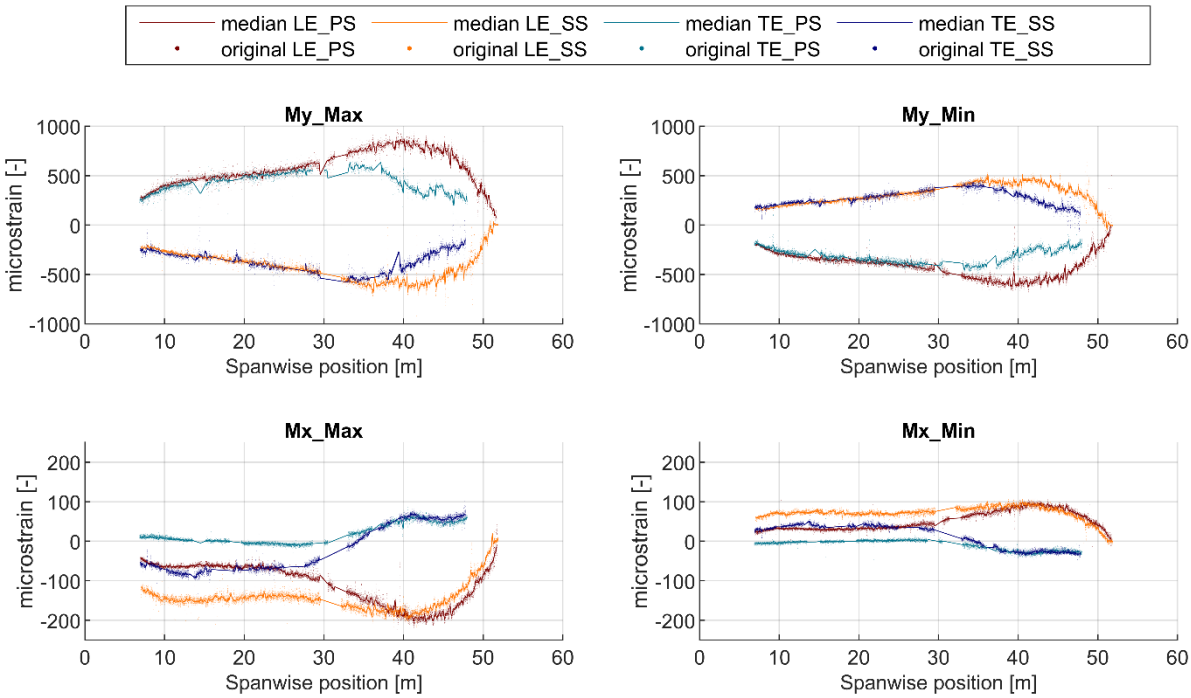

Figure 7. Median data and original data for different load cases

To set the variance into perspective, its square-root (i.e the standard deviation (σ)) is normalized by the median ($\tilde{\mu}$)

$$CV = \frac{\sigma}{\tilde{\mu}} \tag{1}$$

and in the following referred to as Coefficient of Variation (CV). While the Coefficient of Variation is usually calculated by dividing the standard deviation by the mean [6], the version used here is more robust to outliers than the classical version. From **Table 1** one can see, that the average CV over the length of each fiber is lower for the load cases that apply forces in flap-wise (My_Max, My_Min) than in edge-wise (Mx_Max, Mx_Min) direction. It ought to be noted, that the spatially-averaged statistical moments (variance, skewness, kurtosis) over the length of each fiber slightly deviate from those of a normal distribution (**Table 1**) [6].

Table 1. Average statistical moments over all four Fiber Optic Strain Sensors for different load cases

	CV	skewness	kurtosis
My_Max	0,046	0,43	2,75
My_Min	0,043	0,32	2,57
Mx_Max	0,054	0,34	2,71
Mx_Min	0,064	0,32	2,73

After this examination of the statistical properties, the validated FOSS results are exemplarily compared to the FBG results for the My_Min load case. **Figure 9** shows averaged FOSS measurements under maximum force over the span of the wind turbine rotor blade in comparison to the averaged FBG results. The FOSS results are spatially averaged as described above. Furthermore, both FOSS and FBG results are averaged in time over 10 seconds. It becomes clear, that the measured strains on Leading Edge (LE) and Trailing Edge (TE) side are very similar towards the root of the rotor blade and deviate towards the tip of the rotor blade. This is likely due to a coupled flap- and edgewise behavior.

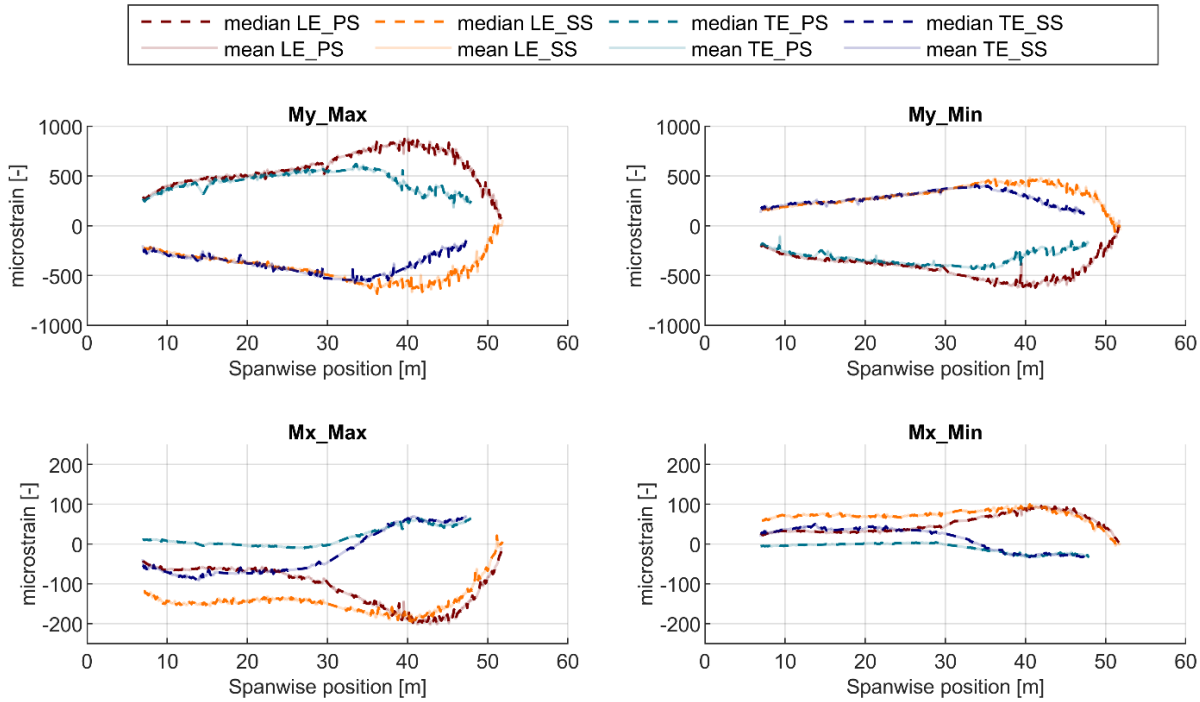

Figure 8. Comparison of median and mean for different load cases

One can also see, that the pressure and suction side strains from FBGs and FOSS match well towards the root while they deviate towards the tip of the blade. It is important to note, that while the span-wise position matches for FBGs and FOSS, the chord-wise position slightly deviates. The difference in measured strain towards the tip of the blade likely results from that.

Furthermore, the Coefficient of Variation (CV) is calculated and plotted in **Figure 9**, the corresponding Y-Axis is on the right side of the plot. Unlike before, where the CV was calculated using samples over 10 cm sections in space, the CV is herein calculated using samples over 10 cm sections in space and 10 seconds in time. While the CV is high at a few sections, the average CV is very low for the FBG sensors ($3.46 \cdot 10^{-10}$) and low for the FOSS ($4.5 \cdot 10^{-3}$).

In summary the post-processed FOSS results and the FBG results are in good agreement. As in previous studies [3,4] the FOSS results are thus considered to be credible.

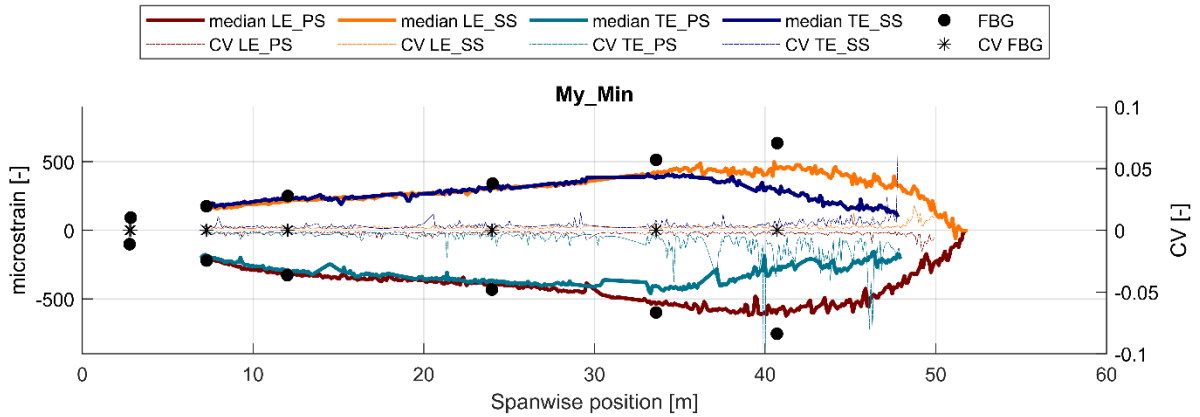

Figure 9. Comparison of measurements from FOSS and FBG for load case My_Min

3.2 Interpretation of strain results

The former subsection shows that the FOSS results are reliable. In light of this, the present subsection gives interpretations of the results. The first use case of the measured and post-processed results is to determine the relation between strain and input force, since this allows to generalize the results. As **Figure 4** shows, the force is applied in increasing (and then decreasing) steps in each load case. Before the force is increased (or decreased) it is held constant for at least 20 seconds. Part of the data from each load step is now used for an averaging in time.
Of the 20 seconds, the first and last part are omitted, to ensure quasi-stationary load conditions. The middle section of each step is used and averaged in time. The averaging in time is done in conjunction with the previously explained averaging in space. In a next step, a linear regression between the averaged strain (time-blocks of 10 seconds, regions of 10 cm) and the averaged input force (time-blocks of 10 seconds) is calculated. The results of this relation between strain and force are shown in **Figure 10**.
It is evident, that the flap-wise (My_Max and My_Min) force normalized strain results are almost axisymmetric with respect to the horizontal axis. This means that the strain response, when pulling in flap-wise direction, only changes sign depending on which side of the rotor blade is rotated towards the ground (My_Max: suction side towards ground; My_Min: pressure side towards ground). The same symmetry is found for the load cases in edge wise direction. In general, the strain response will thus only changes sign (but not amplitude), when the same forces push (instead of pull) on the rotor blade.
In order to assess the quality of the previously calculated linear fit between strain and force, the root mean square error normalized by the respective median value is calculated. The average of this normalized error over the length of each fiber and all load cases is below 5%.

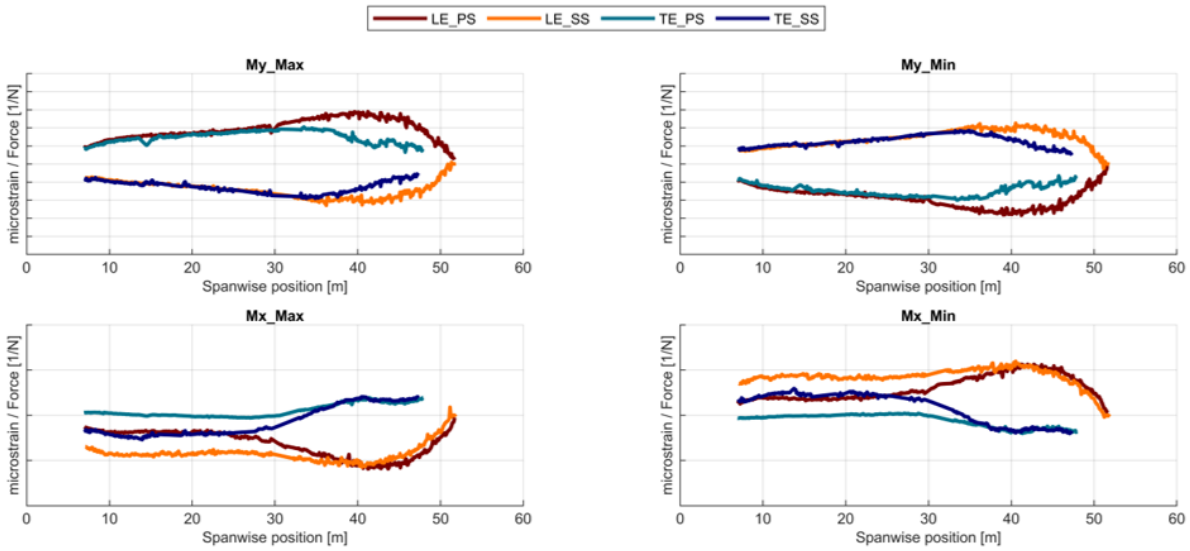

Figure 10. Linear relation between measured strain and force for all fibers and all reference load cases

The small error between the post-processed measurements and the linear strain-force relation over the entire length of each fiber for each reference load case (My_Max, My_Min, Mx_Max, Mx_Min) leads to the assumption that the clamped rotor blade generally behaves like a Euler-Bernoulli (i.e. linear) cantilever beam. The relation between strain and bending moment could then be described as

$$\varepsilon(x) = \frac{\sigma(x)}{EI} = \frac{M(x)c}{EI} \tag{2}$$

Where x is the span-wise coordinate, ε is the strain, σ is the stress, E is Young's Modulus, I is the moment of inertia, M is the bending moment and c is the distance to the neutral axis [7].

By reordering equation (2)

$$\frac{c}{EI} = \frac{\varepsilon(x)}{M(x)} = \frac{\varepsilon(x)}{F\, l(x)} \tag{3}$$

and measuring strain $\varepsilon(x)$, applied forces (F) as well as corresponding lever $l(x)$, the characteristic fraction $\chi = \frac{c}{EI}$ can be determined. This (herein called) characteristic fraction can also be interpreted as the distance to the neutral axis (c) divided by the flexural rigidity (EI). The characteristic fraction χ is material and geometry dependent and changes over the span of the wind turbine rotor blade. Reordering equation (3), leads to a formula that allows to predict bending moments from measured strain

$$M(x) = F\, l(x) = \frac{EI}{c}\varepsilon(x) = \frac{1}{\chi}\varepsilon(x). \tag{4}$$

In order to be able to predict root-bending moments from strain, the characteristic fraction χ is experimentally determined for the previously shown reference load cases (i.e. the force attacking at LF5).

The load is then applied in flap-wise direction at the other four load frames (LF1-LF4) and in edge-wise direction at the load frames LF3 and LF4. This leads to 12 additional load cases (My_Max: 4, My_Min: 4, Mx_Max: 2, Mx_Min: 2) for which the predicted root bending moment (equation (4)) can be compared to the measured value. Each of the load cases consists of multiple load steps, so over 150 bending moment predictions are compared to the measured values. The relative deviation between the measured and predicted root-bending moments is on average 1.6 %. Besides this, in **Figure 11** the characteristic fraction is exemplary shown for one fiber (LE_PS) under My_Max load over the spanwise position. In this the force is attacking in flap-wise direction at each of the five different load-frames (i.e. LF1-LF5). The regions closer (up to 10 % distance in spanwise-coordinate) to the load-frames are omitted. This is because in proximity to the load frame local effects seem to have a notable influence. One can see, that while the force attack point changes, the characteristic fraction in flap-wise direction is in good agreement. The geometry and material dependent characteristic fraction χ can thus be determined experimentally using FOSS. This understanding is crucial for the assessment of existing and design of new wind turbine rotor blades.

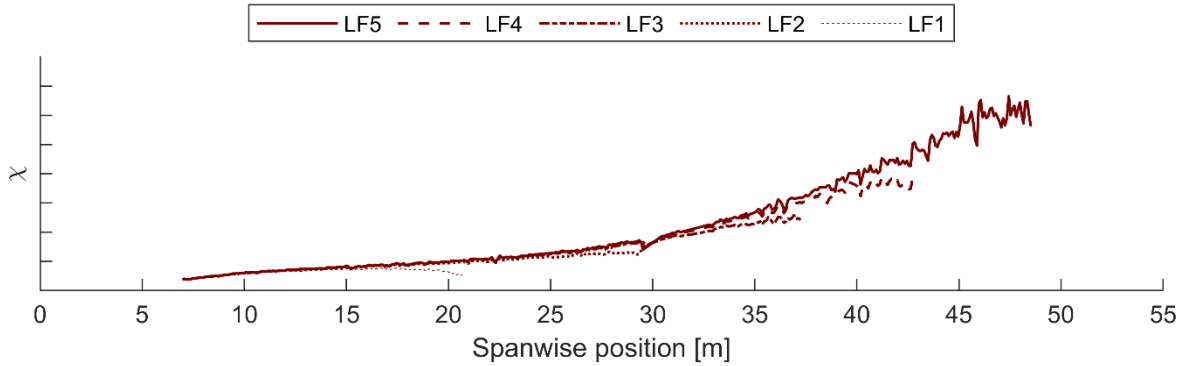

Figure 11. Characteristic fraction χ in flap-wise direction for one fiber (LE_PS) under My_Max loading at different load frames (LF1-LF5)

4. Summary and Outlook

This publication shows high-resolution Fiber-Optic-Strain-Sensor (FOSS) results from static testing of the WiValdi wind turbine rotor blade. The data is post-processed using statistical methods. A comparison of the post-processed FOSS results, with Fiber-Bragg-Grating (FBG) results, shows good agreement. The FOSS results are thus considered valid and their very high spatial resolution makes them particularly relevant for subsequent investigations. Based on these validated results, a linear relation

between strain and input force is determined. The average deviation of the results from this determined relation is generally small (below 5 %). This linearity leads to the assumption, that the rotor blade, behaves similar to a Euler-Bernoulli cantilever beam. Using the Euler-Bernoulli assumption the root-bending moments are predicted with remarkable precision (1.6 % deviation). This prediction is based on two inputs. One input is the experimentally determined characteristic fraction $\chi = \frac{c}{EI} = \frac{\varepsilon(x)}{M(x)}$, in which the distance to the neutral axis (c) is divided by the flexural rigidity (EI). This characteristic fraction is experimentally determined by dividing the strain by the input moment for a set of reference load cases. Besides the characteristic fraction χ, the other input for the bending moment predictions are strain-results. These are measured for the load case, in which the prediction is to be made.
The present work delivers unique high-resolution insight into the stress-strain-relation of a full-scale wind turbine rotor blade and therefore an ideal basis for future investigations. For instance, the results will be used to judge the current structural mechanical state of the wind turbine rotor blade at recurring service inspections. In those future studies, the results of the then to be acquired state and the shown base-line state will be compared. This will enable an understanding of the deterioration of mechanical properties of the wind turbine rotor blade over time. Furthermore, the results allow strain-based deflection predictions as well as validation and updating of the corresponding Finite-Element model. In-spite of requiring extensive post-processing, FOSS measurements are shown to deliver a unique understanding into the mechanical behavior of wind turbine rotor blades and will therefore be used in upcoming measurements on wind turbine rotor blades.

5. References

[1] DLR Forschungswindpark DLR Forschungspark - home (windenergy-researchfarm.com) [last accessed, 13.12.2023]
[2] LUNA Innovations, Optical Distributed Sensor Interrogator, ODiSI 6000 Series | Optical Distributed Sensor Interrogator (lunainc.com) [last accessed, 23.03.2023]
[3] DAVIS, Claire, et al. Evaluation of a distributed fiber optic strain sensing system for full-scale fatigue testing. *Procedia Structural Integrity*, 2016, 2. Jg., S. 3784-3791.
[4] GOVERS, Yves; MEDDAIKAR, Muhammad Yasser; SINHA, Kautuk. Model validation of an aeroelastically-tailored forward swept wing using fiber-optical strain measurements. In: *28th International Conference on Noise and Vibration Engineering, ISMA 2018* S. 1403-1417.
[5] GALKOVSKI, Tena, et al. Fundamental studies on the use of distributed fibre optical sensing on concrete and reinforcing bars. *Sensors*, 2021, 21. Jg., Nr. 22, S. 7643.
[6] ALTMAN, D. G. BS Everitt (1998) Cambridge Dictionary of Statistics.
[7] KO, William L.; RICHARDS, W. Lance; TRAN, Van T. *Displacement theories for in-flight deformed shape predictions of aerospace structures*. 2007.

Acknowledgements

This work was accomplished as part of the research project Deutsche Forschungsplattform für Windenergie (http://dfwind.de) . We greatly acknowledge the financial support of the German Federal Ministry for Economic Affairs and Climate Action, through FKZ 0325936, that enabled this work.

Supported by:

Federal Ministry
for Economic Affairs
and Climate Action

on the basis of a decision
by the German Bundestag